



Solution-based synthesis of efficient WO₃ sensing electrodes for high temperature potentiometric NO_x sensors

Jiun-Chan Yang, Prabir K. Dutta*

Department of Chemistry, The Ohio State University, Columbus, OH 43210-1185, USA

ARTICLE INFO

Article history:

Received 5 August 2008

Received in revised form

19 September 2008

Accepted 19 September 2008

Available online 27 September 2008

Keywords:

Response times

Recovery times

Interfaces

Peroxytungstates

Sensitivity

ABSTRACT

Electrode nanostructures as well as species at electrode–electrolyte interfaces have substantial influence on the sensitivity, response and recovery times of electrochemical sensors. YSZ-based potentiometric NO_x sensors with WO₃ sensing electrodes have shown considerable promise for enhanced sensitivity. In this study, we present a solution-based method using peroxytungstate solutions to fabricate WO₃ electrodes. UV-ozone treatment of the YSZ was necessary for effective bonding of the WO₃ to the YSZ. The resulting WO₃ electrode was found to exhibit different surface nanostructures, better mechanical stability, faster recovery times, and better sensitivity than devices made from conventional ceramic WO₃ powders. Upon UV-ozone treatment, the YSZ surfaces become more reactive towards the acidic peroxytungstate solution and results in monoclinic ZrO₂ formation at the electrode–electrolyte interface, which, based on earlier studies, we propose to be responsible for the improved sensor sensitivity. Better adhesion of the peroxytungstate-based WO₃ electrode to the YSZ electrolyte is related to the improved recovery times.

© 2008 Elsevier B.V. All rights reserved.

1. Introduction

High temperature NO_x sensors have emerged as one of the key elements in combustion industry. Internal combustion engines operated at high air/fuel ratio are currently in development with the goal of increased fuel efficiency. However, in an environment of excess oxygen, three-way catalysts traditionally used to reduce NO_x, hydrocarbon, and CO emissions are not functional. Possible proposed solutions include using a chemical trap with periodic regeneration or reductants for continuous NO_x reduction [1,2]. Reliable NO_x sensors are needed for controlling these processes [3]. Applications of NO_x sensors are also expected in the power, chemical, glass and other high-temperature industries, and as a cross cutting technology in medicine for diagnosing lung diseases.

Most high temperature potentiometric NO_x sensors (>500 °C) in development are based on stabilized zirconia electrolytes and metal oxide electrodes [4–6]. Tungsten trioxide (WO₃), in addition to its applications in electrochromic devices [7] and semiconductor sensors [8,9], has received considerable attention as the electrode material for potentiometric gas sensing. Several reports have described the exceptional NO_x sensing performance when

using WO₃ electrodes with YSZ (yttria-stabilized zirconia), especially at temperatures higher than 600 °C [10–12]. We have reported that non-Nernstian potentiometric sensing devices composed of WO₃ electrodes, YSZ electrolytes, and Pt-loaded zeolite Y (PtY) filters possess unique sensitivity and selectivity toward NO_x [13]. The Pt nanoclusters stabilized in the high surface area microporous zeolite cages exhibit excellent catalytic properties. PtY can also be used as a reference electrode since it is effective in equilibrating NO_x at high temperatures. Our previous study showed that the sensitivity towards NO_x for WO₃-based sensing electrodes is improved due to interfacial reactions at the electrode–YSZ interface, but the recovery times of the sensor was poor [14].

For electrode materials, the structure as well as interfacial species have substantial influence on sensor performance [14–16]. Our previous studies used screen-printing techniques that involved mixing metal-oxide powder with organic binders to fabricate porous metal-oxide electrodes. Ceramic film preparation starting with aqueous peroxy-metal solutions has been used for preparation of metal oxides, including TiO₂ and ZrO₂ [17]. In the present study, peroxytungstate solutions were used to prepare WO₃ sensing electrodes. UV-ozone treatment of YSZ was exploited to increase surface wettability, confine the electrode geometry and provide a lower temperature method to generate the WO₃ layer. Sensors with different electrode structures were characterized by SEM, XRD, and Raman spectroscopy, and their NO₂ sensing performance was evaluated.

* Corresponding author.

E-mail address: dutta.1@osu.edu (P.K. Dutta).

2. Experimental

2.1. Fabrication of basic sensor platforms

The substrate was prepared from YSZ green sheets (3 mol% tetragonal YSZ, NexTech Materials). The 15 mm × 5 mm YSZ green sheets were sintered in air at 1450 °C for 2 h to form dense bodies. Two Pt lead wires (99.95%, 0.13 mm in diameter, Fischer Scientific) were attached to YSZ with a small amount of commercial Pt ink (Englehard, A4731). The end attaching to YSZ was shaped into a disc of 2 mm diameter in order to increase the mechanical stability. The Pt ink was cured at 1200 °C for 2 h to secure bonding between the Pt wire and YSZ. Sensors prepared this way are labeled Sensor A and shown in Fig. 1a.

2.2. Thick WO₃ electrode (Sensor B)

WO₃ powder (99.8%, Alfa Aesar) was mixed with α -terpineol to form a paste, which was then painted on top of the Pt lead wires on the sensor platform (Fig. 1b) The WO₃ layer was spread over as much YSZ as possible. After sintering at 700 °C in air for 2 h, the WO₃ layer was typically about 200 μ m thick.

2.3. Peroxy-complex deposited (PCD) WO₃ electrode on Pt (Sensor C)

Hydrogen peroxide solutions containing 100 mM tungsten were prepared by dissolving tungsten powder (99.99%, Alfa Aesar) in 30% H₂O₂. The pH of the solution was \sim 1. Extra H₂O₂ was decomposed by immersing Pt coils in this solution until bubbling stopped. The solution (denoted as W/H₂O₂ solution) was used to deposit WO₃ films on only the Pt electrodes by immersion coating, since Pt has much higher activity to decompose peroxytungstates than YSZ. After immersing half of the sensor platform into the 100 mM W/H₂O₂ solution for 12 h (as shown schematically in Fig. 2a), the sensor was sonicated and washed thoroughly with deionized water. Heat treatment was then performed at 700 °C in air for 2 h, and the sensor is shown in Fig. 1c.

2.4. Peroxy-complex deposited (PCD) WO₃ electrode on Pt/YSZ (Sensor D)

As shown in Fig. 2b, the sensor platform described previously (Fig. 1a) was treated with UV radiation and ozone for 30 min. The shape of the WO₃ electrode was controlled by confining the UV irra-

diated area on YSZ with a hard mask. Immediately after the UV/O₃ treatment, an aliquot (\sim 20 μ L) of W/H₂O₂ solution was dropped on the radiation treated area and dried in air. The thickness of WO₃ films was 200–600 nm after heating at 700 °C for 2 h. A schematic of this sensor is shown in Fig. 1d.

Additional experiments were conducted in order to understand the influence of UV-ozone treatment and reaction of the highly acidic W/H₂O₂ solution with the YSZ. Tetragonal YSZ powder (Tosoh TZ-3Y) was mixed with the W/H₂O₂ solution to form a suspension with 26 wt% tungsten. The mixture was stirred and dried in a 110 °C oven followed by heat treatment at 700 °C for 2 h. The resulting powder was then characterized by powder diffraction and Raman spectroscopy.

2.5. Pt-loaded zeolite Y reference electrode

Pt-loaded siliceous zeolite Y powder was prepared by ion-exchange. 1.0 g of H⁺ zeolite Y (Si/Al=30, CBV720, Zeolyst International) was added to 2.5 mM [Pt(NH₃)₄]Cl₂ solution followed by stirring for 24 h at room temperature. The Pt-exchanged powder was centrifuged and washed with distilled water. After repeating the ion-exchange process three times, the Pt-exchanged zeolite was calcined at 300 °C for 3 h and exposed to 5% H₂ at 400 °C for 5 h to reduce to metallic Pt. The resulting powder was mixed with α -terpineol and painted on the top of Pt lead wires for all sensors shown in Fig. 1. Heat treatment at 600 °C in air for 2 h was performed to burn out α -terpineol.

2.6. Electrode characterization

FEI XL30 FEG ESEM was used to investigate the microstructure of Pt and WO₃ electrodes. High-resolution SEM micrographs were acquired by FEI Sirion with the through lens detector (TLD). Rigaku Geigerflex X-ray diffractometer with Ni-filtered Cu K α radiation was applied to examine the crystal structure. Raman spectra were collected by HORIBA-Jobin Yvon HR800 spectrometer with laser at 514.5 nm. The cross-section was cut by FEI DB235 focused ion beam. A thick layer of Pt was deposited prior to FIB milling to protect the surface nanostructure.

2.7. Sensing measurements

The gas sensing experiments were performed within a quartz tube placed inside a tube furnace (Lindberg Blue, TF55035A) as in our pervious work [13]. Briefly, a computer-controlled gas delivery

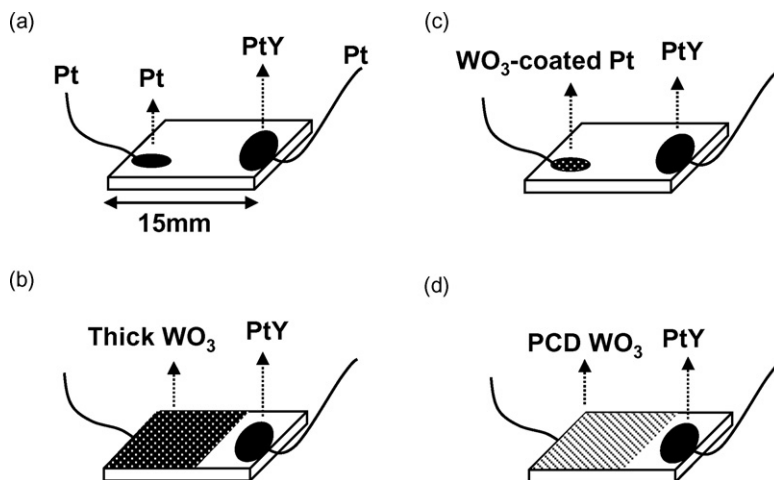


Fig. 1. Potentiometric sensors composed of YSZ electrolyte and Pt-zeolite Y coated/Pt reference electrodes. Sensing electrodes in (a) Pt (Sensor A), (b) commercial WO₃ powder (Sensor B), (c) peroxytungstate solution on Pt only (Sensor C) and peroxytungstate solution on UV/ozone treated YSZ (Sensor D) (PCD = peroxy-complex deposition).

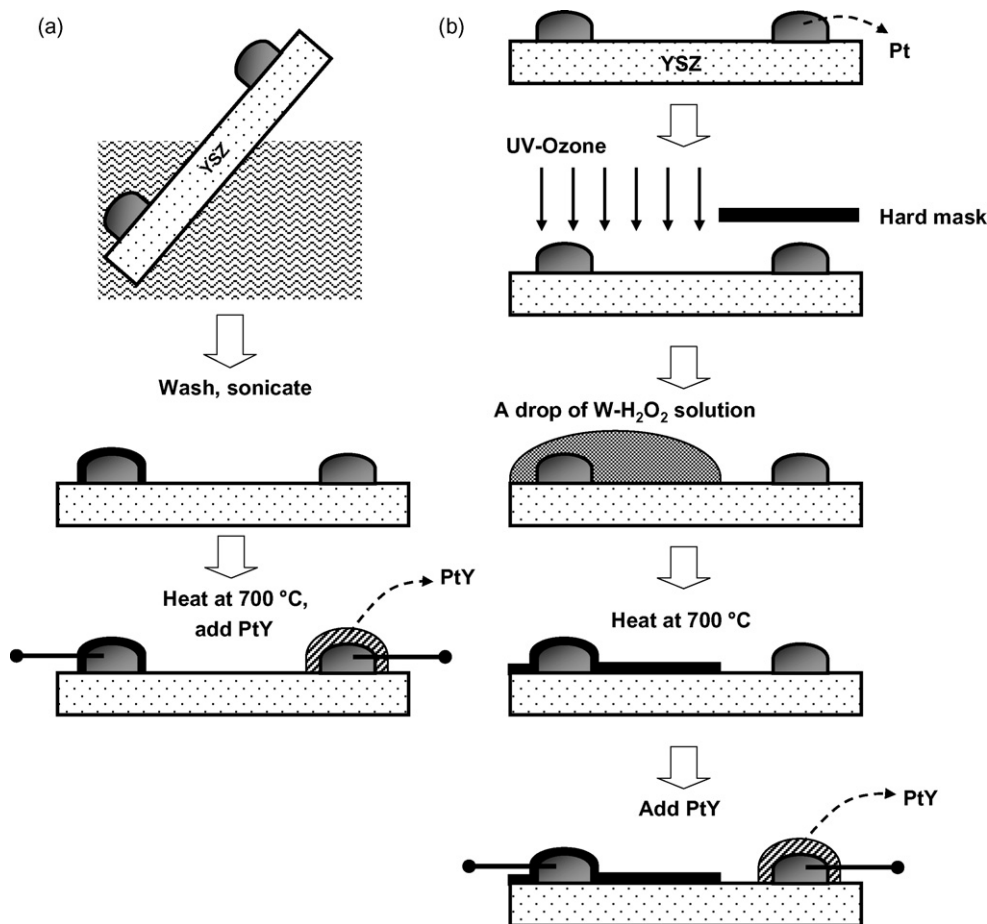


Fig. 2. Schematic representation of the fabrication process of (a) Sensor C and (b) Sensor D with peroxytungstate solutions.

system with calibrated mass flow controllers (MFC) was used to introduce the test gases. Four certified N_2 -balanced NO_x cylinders (30 ppm NO , 30 ppm NO_2 , 2000 ppm NO , and 2000 ppm NO_2 , Prax-air) were used as NO_x sources. Sensor tests were carried out with mixtures of dry air, NO_2 , and nitrogen with total gas flow rates of $200\text{ cm}^3/\text{min}$ at 600°C . The open circuit potential of sensors was recorded by Hewlett-Packard 34970A data acquisition system with $10\text{ G}\Omega$ internal impedance. The sensor devices were conditioned in a 600°C furnace in air for 15 h prior to performing sensor tests.

3. Results

3.1. Sensor fabrication and characterization

The four electrochemical sensors used in this study are illustrated in Fig. 1. All sensors are based on the same platform with different sensing electrodes, but the same reference electrode (Pt-zeolite Y/Pt). Of particular interest are sensors C and D prepared with the peroxytungstate solutions, the procedure depicted schematically in Fig. 2.

Fig. 3a shows the morphology of the Pt electrode (Sensor A) after sintering at 1200°C . The Pt ink used in this work resulted in a dense structure on the YSZ surface. The surface morphology of WO_3 thick films (commercial powder) painted on the Pt electrodes and after heat treatment in 700°C for 2 h (Sensor B) is shown in Fig. 3b. The thickness is around $100\text{--}200\ \mu\text{m}$ and the grain size of WO_3 is $300\text{--}500\text{ nm}$.

With Sensor C, after immersing in the W/H_2O_2 solution for 12 h and sonicating in water for 5 min (Fig. 2a), a layer of tungsten com-

pounds (identified by EDS), most likely tungsten hydroxide, was observed only on the Pt surface. No deposit of W compounds was found on YSZ after sonication by SEM or EDS. The layer on the Pt was amorphous and did not show any characteristic peaks in XRD. Heat treatment at 700°C led to the formation of WO_3 , the SEM of which is shown in Fig. 3c and covers the Pt (same substrate as in Fig. 3a); the microstructure of WO_3 is clearer in the magnified image of Fig. 3d. The grain size is about $100\text{--}200\text{ nm}$ and the film covered the Pt surface uniformly. Fig. 3e shows the SEM of the WO_3 /Pt/YSZ interface, and Fig. 3f is the same cross-section at a higher magnification. It is evident that a layer is formed uniformly on the Pt, with the thickness of the WO_3 layer being about 200 nm . The powder diffraction pattern in Fig. 4a clearly indicates the presence of monoclinic WO_3 .

The original surface of YSZ was too hydrophobic to form a uniform WO_3 coating with aqueous W/H_2O_2 solutions. Sensor D was prepared by UV-ozone treatment of the Pt/YSZ to make the surface more hydrophilic, followed by treatment with the W/H_2O_2 solution (Fig. 2b). Upon heating to 700°C , the WO_3 formed had much better adhesion on YSZ than the thick WO_3 film (Sensor B), since the latter could be readily removed by sonication in water. The morphology of the WO_3 formed on YSZ is shown in Fig. 3g. The thickness of the film was around $100\text{--}300\text{ nm}$. Without the UV-ozone treatment, W/H_2O_2 solution did not interact with the YSZ.

The XRD in Fig. 4b was acquired from the WO_3 film from commercial powder on the YSZ substrate (Sensor B). Fig. 4c shows the diffraction of the WO_3 formed by the peroxytungstate/UV-ozone treatment (Sensor D). Comparing with Fig. 4b, two significant differences are noted. First, the WO_3 (100) peak ($2\theta = 24.23^\circ$) has higher intensity than (001) and (010) peaks ($2\theta = 22.91$ and

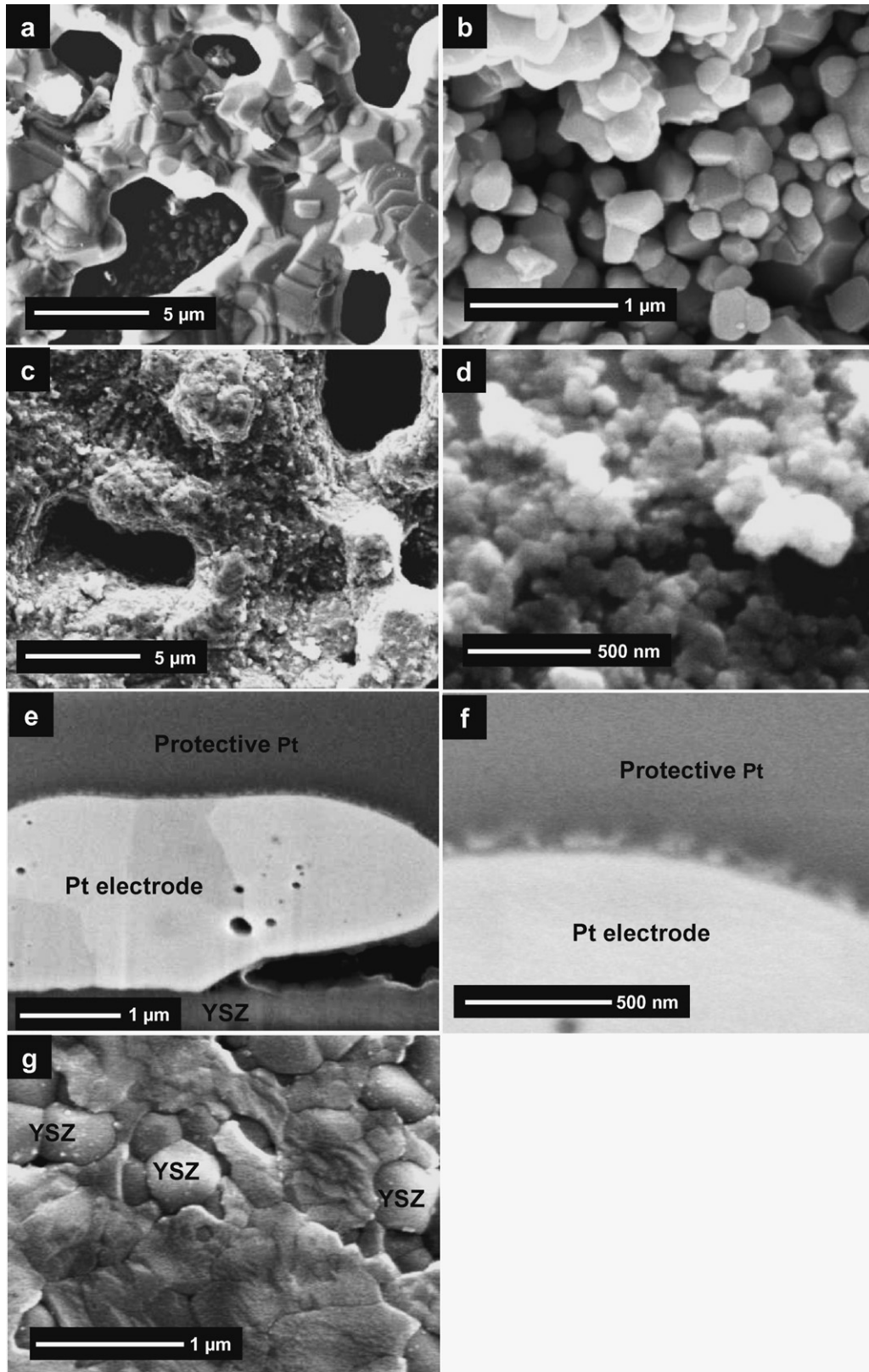


Fig. 3. SEM micrographs: (a) bare Pt electrode (used in Sensor A), (b) 700 °C treated commercial WO_3 powder (Sensor B), (c) and (d) peroxytungstate-coated Pt electrodes heated in air at 700 °C for 2 h (Sensor C); (e) cross-section of the $\text{WO}_3/\text{Pt}/\text{YSZ}$ interface (Sensor C); (f) higher magnification micrograph of the FIB-cut cross-section of $\text{WO}_3/\text{Pt}/\text{YSZ}$, protective Pt was deposited in advance, (Sensor C); (g) peroxytungstate-based WO_3 on UV-ozone treated YSZ after 700 °C treatment.

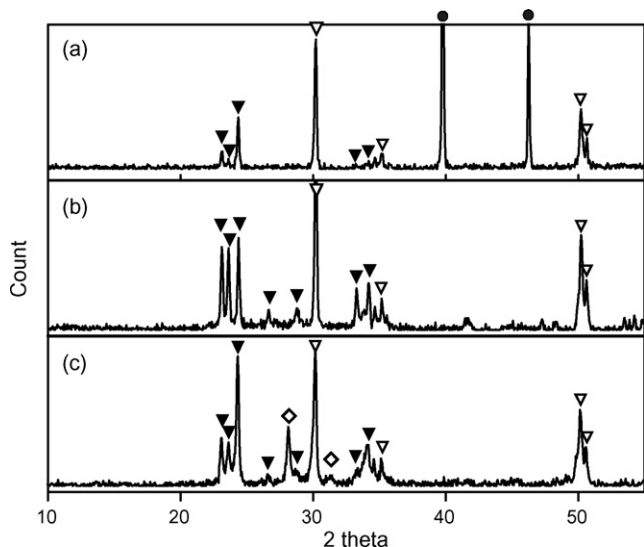


Fig. 4. Room temperature XRD: (a) WO_3 -coated platinum electrode on YSZ after 700°C treatment (Sensor C). (b) Commercial WO_3 powder on YSZ after 700°C treatment (Sensor B). (c) peroxytungstate-based WO_3 deposited on UV-ozone treated YSZ after 700°C treatment (Sensor D). Symbols: (▼) Monoclinic WO_3 , (▽) Tetragonal YSZ, (◇) Monoclinic ZrO_2 , (●) Cubic Pt.

23.48° , respectively), which possibly implies some texturing. Second, the two peaks at $2\theta = 28.17$ and 31.47° indicates the formation of monoclinic ZrO_2 .

Fig. 5 shows the Raman spectra of WO_3 (Plot a), tetragonal YSZ (Plot b), and monoclinic ZrO_2 (Plot c) and from the sensing electrode for Sensor D (plot d). Plot (d) exhibits features from all three species, which is consistent with the XRD result in Fig. 4.

3.2. NO_2 sensing behavior

Fig. 6 compares the EMF– $\log(\text{NO}_2)$ plots for Sensor A to D at 600°C . Plot (a) shows that Pt electrode (sensor A) has lower NO_x signal than any of the devices containing WO_3 and the measured EMF is not in logarithmic relation to NO_2 concentration. The signal

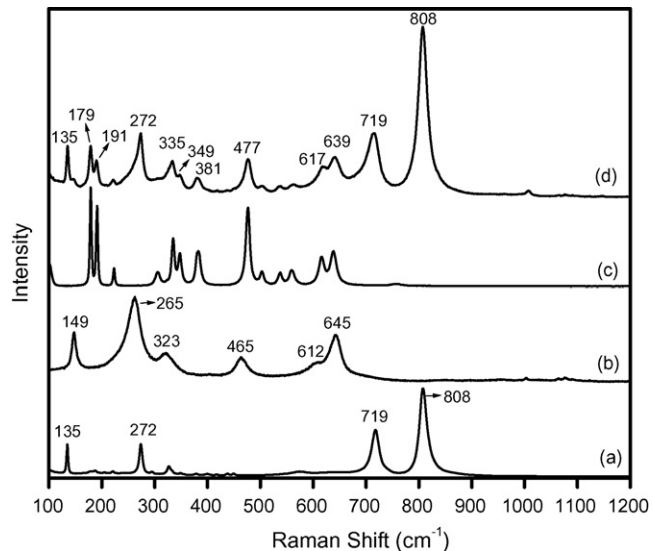


Fig. 5. Raman spectra (a) 700°C treated commercial WO_3 powder, (b) tetragonal YSZ, (c) monoclinic ZrO_2 , (d) peroxytungstate-based WO_3 deposited on UV-ozone treated YSZ with 700°C treatment (Sensor D).

from WO_3 -coated Pt electrode also does not obey a logarithmic relation to NO_2 concentration (plot c). With peroxytungstate/UV-ozone treatment WO_3 electrode, the signal of Sensor D (Plot d) exhibits logarithmic relation to NO_2 concentration from 40 to 800 ppm. Compared with the thick WO_3 electrodes from commercial powder (Sensor B), the major improvement in Sensor D is the better response and recovery times, as shown in Fig. 7 for 40–800 ppm NO_2 in 3% O_2 . For 110 ppm NO_2 , the 90% response time was 45 s and the recovery time was 120 s.

4. Discussion

In an earlier publication, we investigated in detail the use of commercial WO_3 powder as a sensing electrode and concluded that its superior performance was related to the formation of interfacial

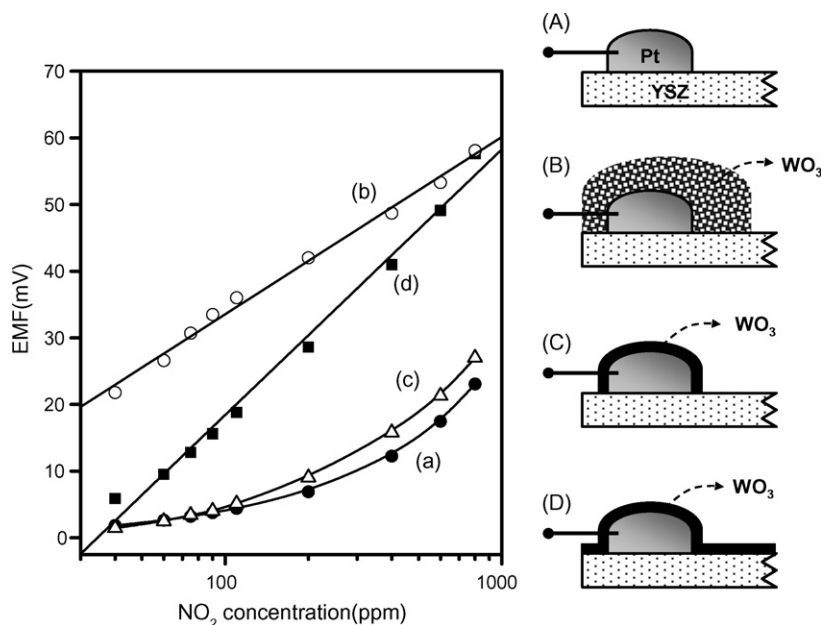


Fig. 6. Schemes and EMF– $\log[\text{NO}_2]$ plots of sensors illustrated in Fig. 1. Plots (a) through (d) represent Sensors A, B, C and D.

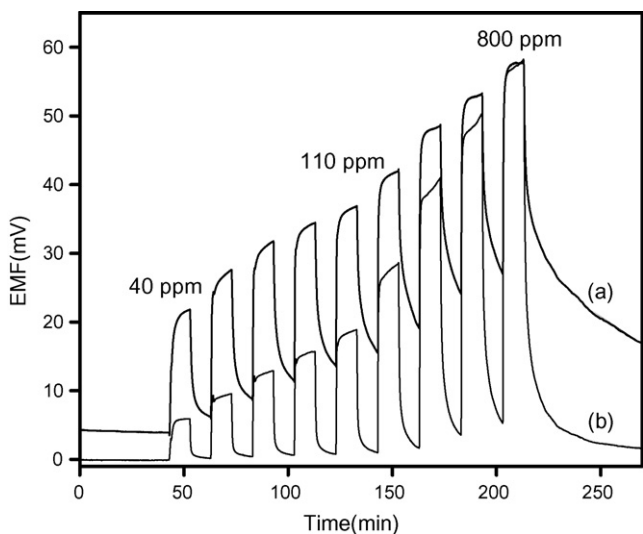
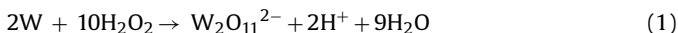


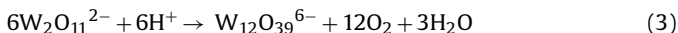
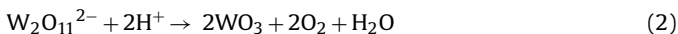
Fig. 7. Signal transients in 3% oxygen and 40–800 ppm NO₂ at 600 °C from (a) Sensor B, (b) Sensor D (40, 60, 75, 90, 110, 200, 400, 600 and 800 ppm).

zirconia and yttrium tungstates that minimized the heterogeneous equilibration of the NO_x species [14]. We also noted that the recovery times of the sensors were poor, which motivated us to do the present study. Clearly, an improvement in sensor performance was noted with the electrodes prepared via the peroxytungstate/UV-ozone treatment (Fig. 7b) and forms the basis of this discussion. The choice of the Pt-zeolite/Pt as the reference electrode has been discussed in earlier studies [13].

Peroxytungstates are formed from the reaction between H₂O₂ and tungsten. H₂O₂ acts as both an oxidant and a complexing agent. The dominant peroxytungstate species in acidic solutions is reported to be W₂O₁₁²⁻. This anion is formed by the following reaction [18]:



Peroxytungstates are thermodynamically unstable and decompose via several reaction pathways, generating polytungstates and WO₃:



Peroxytungstate solutions have been used to deposit WO₃ thin films by electrodeposition [18–20]. The advantage of using the peroxy-complex solution for deposition is that there are no other anions involved in the reaction, so no effort is needed to remove anionic species.

For Sensor C, because Pt is a good catalyst to decompose H₂O₂ and peroxytungstate species, immersing the Pt electrode into the peroxytungstate solution resulted in the formation of a tungsten hydroxide layer on the surface of Pt electrodes. The layer adhered very well on Pt electrodes and could be converted to WO₃ by heat treatment. However, the improvement in sensor performance as compared to Pt (Plot c in Fig. 6) is minimal, indicating the importance of the WO₃-YSZ interface for the sensing reaction.

We previously reported that monoclinic phase ZrO₂ was observed from WO₃-YSZ mixtures treated at 950 °C [14]. In that case, yttrium tungsten oxides were also identified. In Fig. 4, the formation of monoclinic phase ZrO₂ is evident, along with WO₃. Raman spectra in Fig. 5 are also consistent with the XRD data. Peaks at 179, 191, 335, 349, and 477 cm⁻¹ in Plot (d) support the formation of monoclinic ZrO₂. Three intense peaks at 272, 719, and 808 cm⁻¹

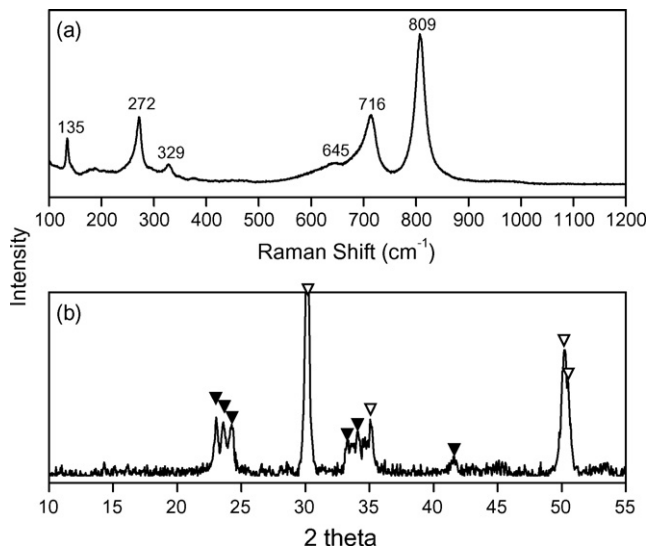


Fig. 8. Raman spectra (a) and XRD (b) of a mixture of W/H₂O₂ solution and tetragonal YSZ powder after heat treatment at 700 °C for 2 h (W content of mixture was 26 wt%). XRD Symbols: (▼) Monoclinic WO₃, (▽) Tetragonal YSZ.

indicate crystalline WO₃ [21–23]. Since previous studies have shown that heating the WO₃-YSZ mixture in air to 700 °C did not result in the formation of monoclinic ZrO₂ (at least not detectable by XRD), the reaction pathway with the peroxytungstate/UV-ozone treatment is possibly different from reaction of YSZ with WO₃, as proposed previously [14]. It is important to note that peroxytungstate solutions have been used to deposit WO₃ on glass and silicon wafers without UV-ozone treatment [24].

In order to understand the origin of the monoclinic ZrO₂, the influence of H₂O₂ and UV-ozone treatment was examined. A YSZ sheet was immersed into 30% H₂O₂ for 12 h and another one was treated with UV-ozone for 30 min. No monoclinic ZrO₂ was identified on either sheet (data not shown). The peroxy-complex is formed in a strongly acidic solution. It is possible that YSZ may dissolve in the acidic peroxide solution and lead to the formation of monoclinic ZrO₂. To examine this possibility, tetragonal YSZ powder was mixed with the acidic W/H₂O₂ solution and the solid heated at 700 °C for 2 h. The XRD and Raman data in Fig. 8 does not show any characteristic peaks from monoclinic ZrO₂. This implies that YSZ is chemically resistant to the peroxytungstate solution.

Hence, the formation of monoclinic ZrO₂ must be due to a combined effect of the UV-ozone treatment and acidic peroxytungstate solutions. The reactive oxygen radicals can attack the YSZ surface, resulting in a hydrophilic hydroxyl-terminated surface, which then reacts with the peroxytungstate solution and forms WO₃ and monoclinic ZrO₂. Our original intent for the UV-ozone treatment was to increase the wettability of YSZ. However, this treatment also makes the YSZ more reactive to the peroxytungstates. From a fabrication viewpoint, the solution based peroxytungstate/UV-ozone method should lead to better control of the thickness and geometry of electrode deposition as compared to the screen-printing method with WO₃ powders. Also, the area of electrode deposition can be controlled precisely by the area of UV-ozone treatment. The process described in this study is more likely to lead to consistent and reproducible sensors, not to mention the fast response times required for feedback control.

In our previous study with commercial WO₃ powders, the interfacial reaction between WO₃ and YSZ led to the formation of yttrium tungsten oxides and ZrO₂ [14]. Based on chemical reactivity studies, we proposed that the increase in sensitivity was due to these interfacial species that minimized the chemical equilibration

of the NO_x species on the WO_3/YSZ interface, and therefore resulted in a stronger electrochemical signal. We noted the poor recovery times of these sensors, but did not offer any explanation. Based on the present study, we conclude that the interfacial species (ZrO_2) does improve the sensitivity, as we had noted earlier. Figs. 6 and 7 show that at low concentrations of NO_2 , the commercial powder does have higher sensitivity than the peroxy-based generation of WO_3 ; this could arise from the smaller particles of WO_3 in the peroxy-case (compare Fig. 3b and d) which promotes the heterogeneous catalytic NO_x equilibration reaction. However, the bonding of the WO_3 electrode to the Pt/YSZ via the peroxy method is considerably stronger than the electrodes made with the commercial WO_3 powder (Sensor B, WO_3 layer can be removed by sonication). The stronger bonding will facilitate the electronic communication between the electrode and electrolyte, and we propose is the reason for the improved response/recovery times (Fig. 7). Thus, both the interfacial species and strong electrode–electrolyte bonding are necessary for improved sensor performance.

5. Conclusions

Aqueous peroxytungstate solutions were used to fabricate WO_3 sensing electrodes for high temperature potentiometric NO_x sensing. WO_3 films can be deposited selectively on Pt electrodes only or on both Pt electrodes and UV-ozone treated YSZ by immersion coating or drop coating. The WO_3/YSZ sensing electrode fabricated by this method has better mechanical stability, higher sensitivity, and better response/recovery times than devices fabricated from commercial WO_3 powder. From the XRD and Raman results, monoclinic ZrO_2 was found on the electrode surface even at heat treatment temperatures as low as 700°C . This is due to the combined effect of acidic peroxytungstate solutions and the UV-ozone treatment, since neither one alone causes this phenomenon. We propose that the sensitivity is improved due to the ZrO_2 at the interface and fast recovery times is due to the stronger bonding of the WO_3 to the YSZ electrolyte. This study provides a simple and practical option for fabricating metal oxide electrodes via solution chemistry.

Acknowledgements

This work was supported by the Department of Energy (DE-FC26-03NT41615). The authors thank Dr. Jing-Jong Shyue for his assistance on FIB and Professor Umit Ozkan for access to Raman instrumentation.

References

- [1] M. Shelef, Selective Catalytic Reduction of NO_x with N-Free Reductants, *Chem. Rev.* 95 (1995) 209–225.
- [2] L. Olsson, H. Persson, E. Fridell, M. Skoglundh, B. Andersson, Kinetic study of NO oxidation and NO_x storage on Pt/ Al_2O_3 and Pt/ $\text{BaO}/\text{Al}_2\text{O}_3$, *J. Phys. Chem. B* 105 (2001) 6895–6906.
- [3] N. Docquier, S. Candel, Combustion control and sensors: a review, *Prog. Energy Combust. Sci.* 28 (2002) 107–150.
- [4] F. Menil, V. Coillard, C. Lucat, Critical Review of nitrogen monoxide sensors for exhaust gases of lean burn engines, *Sens. Actuators, B* 67 (2000) 1–23.
- [5] N. Miura, G. Lu, N. Yamazoe, Progress in mixed-potential type devices based on solid electrolyte for sensing redox gases, *Solid State Ionics* 136 (2000) 533–542.
- [6] K. Hamamoto, Y. Fujishiro, M. Awano, Gas Sensing Property of the electrochemical cell with a multilayer catalytic electrode, *Solid State Ionics* 179 (2008) 1648–1651.
- [7] J. Livage, D. Ganguli, Sol-gel electrochromic coatings and devices: A review, *Sol. Energy Mater. Sol. Cells* 68 (2001) 365–381.
- [8] I. Jimenez, J. Arbiol, G. Dezaneeu, A. Cornet, J.R. Morante, Crystalline structure, defects and gas sensor response to NO_2 and H_2S of tungsten trioxide nanopowders, *Sens. Actuators, B* 93 (2003) 475–485.
- [9] S. Santucci, L. Lozzi, M. Passacantando, S. Di Nardo, A.R. Phani, C. Cantalini, M. Pelino, Study of the surface morphology and gas sensing properties of WO_3 thin films deposited by vacuum thermal evaporation, *J. Vac. Sci. Technol., A* 17 (1999) 644–649.
- [10] G. Lu, N. Miura, N. Yamazoe, Stabilized zirconia-based sensors using WO_3 electrode for detection of NO or NO_2 , *Sens. Actuators, B* 65 (2000) 125–127.
- [11] A. Dutta, N. Kaabbuathong, M.L. Grilli, E. Di Bartolomeo, E. Traversa, Study of YSZ-based electrochemical sensors with WO_3 electrodes in NO_2 and CO environments, *J. Electrochem. Soc.* 150 (2003) H33–H37.
- [12] J. Yoo, S. Chatterjee, E.D. Wachsman, Sensing Properties and selectivities of a $\text{WO}_3/\text{YSZ}/\text{Pt}$ potentiometric NO_x sensor, *Sens. Actuators, B* 122 (2007) 644–652.
- [13] J.-C. Yang, P.K. Dutta, Promoting selectivity and sensitivity for a high temperature YSZ-based electrochemical total NO_x sensor by using a Pt-loaded zeolite Y filter, *Sens. Actuators, B* 125 (2007) 30–39.
- [14] J.C. Yang, P.K. Dutta, Influence of solid-state reactions at the electrode–electrolyte interface on high-temperature potentiometric NO_x -gas sensors, *J. Phys. Chem. C* 111 (2007) 8307–8313.
- [15] S. Zhuiykov, T. Ono, N. Yamazoe, N. Miura, High-temperature NO_x sensors using zirconia solid electrolyte and zinc-family oxide sensing electrode, *Solid State Ionics* 152 (2002) 801–807.
- [16] L.P. Martin, A.Q. Pham, R.S. Glass, Effect of Cr_2O_3 electrode morphology on the nitric oxide response of a stabilized zirconia sensor, *Sens. Actuators, B* 96 (2003) 53–60.
- [17] Y.F. Gao, K. Koumoto, Bioinspired ceramic thin film processing: Present status and future perspectives, *Cryst. Growth Des.* 5 (2005) 1983–2017.
- [18] E.A. Meulenkamp, Mechanism of WO_3 electrodeposition from peroxytungstate solution, *J. Electrochem. Soc.* 144 (1997) 1664–1671.
- [19] S.H. Baek, K.S. Choi, T.F. Jaramillo, G.D. Stucky, E.W. McFarland, Enhancement of photocatalytic and electrochromic properties of electrochemically fabricated mesoporous WO_3 thin films, *Adv. Mater.* 15 (2003) 1269.
- [20] T. Pauporte, Y. Soldo-Olivier, R. Faure, XAS study of amorphous WO_3 formation from a peroxytungstate solution, *J. Phys. Chem. B* 107 (2003) 8861–8867.
- [21] S. Kuba, P.C. Heydorn, R.K. Grasselli, B.C. Gates, M. Che, H. Knozinger, Redox properties of tungstated zirconia catalysts: Relevance to the activation of n-alkanes, *Phys. Chem. Chem. Phys.* 3 (2001) 146–154.
- [22] D.G. Barton, M. Shtein, R.D. Wilson, S.L. Soled, E. Iglesia, Structure and electronic properties of solid acids based on tungsten oxide nanostructures, *J. Phys. Chem. B* 103 (1999) 630–640.
- [23] M. Scheithauer, R.K. Grasselli, H. Knozinger, Genesis and structure of WO_x/ZrO_2 solid acid catalysts, *Langmuir* 14 (1998) 3019–3029.
- [24] G. Leftheriotis, S. Papaefthimiou, P. Yianoulis, A. Siokou, D. Kefalas, Structural and electrochemical properties of opaque sol-gel deposited WO_3 layers, *Appl. Surf. Sci.* 218 (2003) 275–280.

Biographies

Jiun-Chan Yang completed his undergraduate studies in Taiwan and received his PhD in chemistry in 2007 from the Ohio State University. He is currently a postdoctoral fellow at Northwestern University.

Prabir K. Dutta received his PhD degree in chemistry from Princeton University. After four years of industrial research at Exxon Research and Engineering Company, he joined The Ohio State University, where currently he is professor of chemistry. His research interests are in the area of microporous materials, including their synthesis, structural analysis and as hosts for chemical and photochemical reactions.